

Programmable Load with Real-Time Data Logging and Load Profiling for DC-DC Converters and Renewable Sources

Swathi Hatwar H., Anup Shetty, and Suryanarayana K.*

Department of Electrical and Electronics Engineering, NITTE (Deemed to be University),
NMAM Institute of Technology, Nitte-574110, India

Email: hswathihatwar@nitte.edu.in (S.H.H.), anup.shetty@nitte.edu.in (A.S.), suryanarayana@nitte.edu.in (S.K.)

Manuscript received January 24, 2025; revised March 9, 2025; accepted March 13, 2025

*Corresponding author

Abstract—The validation of renewable energy systems and battery technologies is challenging due to the dynamic and non-ideal behaviour of real-world loads. This study presents a programmable load solution designed to emulate such loads using FET switches and passive components, controlled by an STM32 microcontroller for precision and reliability. The system operates in multiple modes, including Constant Current (CC), Constant Voltage (CV), Constant Resistance (CR), Constant Power (CP), and energy source profiling with a maximum voltage of 100V and current capacity of 50A, incorporating overcurrent and overvoltage protection for safety. It supports the validation of diverse power sources such as Switched-Mode Power Supplies (SMPS), battery chargers, and renewable energy systems, while providing real-time data logging and remote monitoring for detailed analysis. This solution reduces testing time and costs by enabling efficient, automated testing and characterization, offering flexibility for various scenarios and ensuring the quality, reliability, and performance of DC-DC converters and renewable energy systems.

Index Terms—DC-DC Converter testing, Renewable energy system characterization, battery characterization, STM32-based control system, real-time data logging

I. INTRODUCTION

With the growing emphasis on green energy and sustainable technologies, the demand for reliable Power Supply Units (PSUs), efficient battery systems, and renewable energy sources is increasing [1]. Technological advances have driven the demand for compact, efficient, and high-performance PSUs to power a wide range of applications, from consumer electronics to industrial systems. Similarly, the transition towards cleaner energy solutions has accelerated the development of renewable energy systems, such as solar panels and wind turbines, along with advanced battery technologies for energy storage [2]. These systems must deliver a consistent performance and operate efficiently under varying and unpredictable real-world conditions. Accurate testing and validation of these systems is crucial to ensure their reliability, safety, and compliance with performance standards. Traditionally, testing is conducted using fixed resistors or rheostats. However, selecting appropriate resistive loads for every design can be a tedious and time-

consuming task because the resistor values often vary based on the design requirements. Additionally, testing for different load currents to evaluate the system performance typically requires multiple rheostats connected in parallel or series, which further complicates the process. These limitations of physical resistive loads can be effectively addressed by replacing them with semiconductor switches that are configured to operate as electronically controlled resistive loads, called electronic loads [3]. Advancements in semiconductor technology, particularly in power devices, such as MOSFETs and IGBTs, have facilitated the design of programmable loads capable of emulating diverse load conditions. These programmable loads provide a controlled environment for testing PSUs, batteries, and renewable energy sources, enabling evaluation of their performance, efficiency, and durability under various scenarios [4, 5].

An electronic load (e-load), also known as a power absorber or programmable load, is a device used to sink current from various energy sources such as conventional power supplies, batteries, PV arrays, and fuel cells [6]. It acts as a controllable load, enabling the simulation of real-world operating conditions for these sources [7]. When designing a power source, the load is essential for system validation. Conventional testing methods often rely on fixed resistive loads that absorb current from the source. Although suitable for open-loop applications where the load remains constant and does not require adaptation to changing conditions, resistive loads are inadequate for closed-loop systems that demand dynamic load adjustments based on real-time feedback to meet specific performance criteria. Additionally, for complex testing scenarios that require validation under varying operating states, resistive loads are not an optimal solution. Adjusting fixed resistive loads is time consuming, requires multiple resistors, switching control mechanisms, and dedicated control software, and often fails to emulate actual devices connected to power sources in practical applications.

Resistive loads also lack the ability to control or limit the current and voltage consumed, which necessitates special precautions to prevent potential damage to the system. These limitations can be overcome using

programmable e-loads, which offer high flexibility to sink currents under varying power profiles and operate in multiple modes. Programmable e-loads provide a more effective solution for device testing than fixed resistors, emulating conventional loads with high precision and control.

An electronic load based on the boost topology to realize the function of constant current mode for a small current range and low-power applications is discussed in [8]. The boost converter topology is preferable to the buck converter because of its low ripple current, as the input current is continuous in nature for a large value of inductance in boost and discontinuous input current in the buck converter. The design offers a high control accuracy, continuous input current, and good performance in terms of steady accuracy, voltage regulation, and load regulation. However, this study focuses solely on the constant current mode and does not address potential challenges in scaling up the design for high-power applications or discussing any thermal management considerations that might become critical at higher power levels.

A comprehensive study on the design and modeling of a low-cost Direct-Current (DC) analog electronic load was highlighted in [9]. The detailed design procedure and operational principles were also discussed. The design is capable of operating in the constant current mode and is demonstrated through various test scenarios, including battery discharge curve analysis and noise measurement in switched power supplies. However, the design is limited to low-power ratings and requires manual control through a potentiometer. In addition, it can operate only in the constant-current mode.

The design and implementation of a Programmable Electronic Load (PEL) for aerospace vehicle testing were presented in [10]. The system uses five linear MOSFETs in parallel, and can handle up to 500 Watts of power. MOSFETs were controlled using a microcontroller (MSP430F6659). However, the research does not have provision for real-time data logging limiting future analysis capability.

The electronic load technique, implemented using a MOSFET, was compared with the capacitive load method for tracking the I - V and P - V characteristics of polycrystalline and monocrystalline solar panels in [11, 12]. Utilizing low-cost components and Arduino-based data acquisition, the study demonstrated the electronic load technique's superior ability to deliver precise and rapid measurements. Additionally, the integration of capacitive and electronic load techniques was proposed to enhance performance by increasing data density and reducing plotting time, making the approach particularly effective for defect detection and analyzing external parameters. However, the study's scope was limited to two panel types, and all testing was conducted under standard test conditions. Despite these limitations, the findings underscore the potential of these techniques for efficient and cost-effective solar panel characterization and diagnostics, with significant implications for improving system performance and maintenance.

Despite significant advancements in electronic loads for power source testing, several limitations remain

unaddressed in existing studies. Most designs focus on low-power applications without addressing scalability challenges for high-power systems, particularly in terms of thermal management, efficiency, and control stability. Existing studies also primarily emphasize constant current mode, neglecting other essential operating modes which are necessary for comprehensive power source testing. To address these limitations, an electronic load capable of real-time data logging and load profiling was developed, enabling a detailed analysis of the power source's behaviour over time. The system is equipped with precision current and voltage measurement capabilities, allowing for accurate monitoring of power source performance under different load conditions. It supports dynamic load testing by varying the resistance, current, or power, based on the selected mode of operation. Additionally, these features are critical for assessing the efficiency, stability, and reliability of power sources in various applications including renewable energy systems, battery testing, and power conversion systems. The use of advanced control algorithms ensures that the load response is fine-tuned to match the requirements of the test device, thereby providing precise control for each test scenario.

The remainder of this paper is organized as follows: Section II outlines the detailed architecture of the programmable load and explains the functionality of each block. Section III discusses the selection and roles of the individual components, including current and voltage measurement circuits, along with their implementation. It also covers microcontroller selection and provides a comprehensive explanation of the software implementation. Section IV focuses on the hardware implementation of the programmable load and highlights its various modes of operation, including the testing of the SMPS and characterization of PV panels. Finally, Section V presents the conclusions of this study.

II. SYSTEM DESIGN AND ARCHITECTURE

A. Components of Programmable Load

The major components include power FET switches, operational amplifiers, sense resistors, signal conditioning circuits, and a digital controller. The voltage from the power source is fed to the transistor bank. The transistor bank was controlled through a digital controller that controlled the gate voltage of the FET. The controller is programmed based on the test requirement, which is user-configurable. The unit monitors the current, voltage, resistance, and power displayed in the front panel. The system can be operated under different modes selected by the switch and rotary encoder. These mode selections are performed based on the test setup.

B. System Block Diagram

The system comprises of three linear MOSFETs connected in parallel to handle the required load current. The total current passing through the MOSFETs was measured using a shunt resistor, whereas the supply voltage was measured using a potential divider circuit. Both the measured current and voltage signals are fed to the Analog to Digital Converter (ADC) pins of the

microcontroller via a signal-conditioning circuit, as shown in Fig. 1.

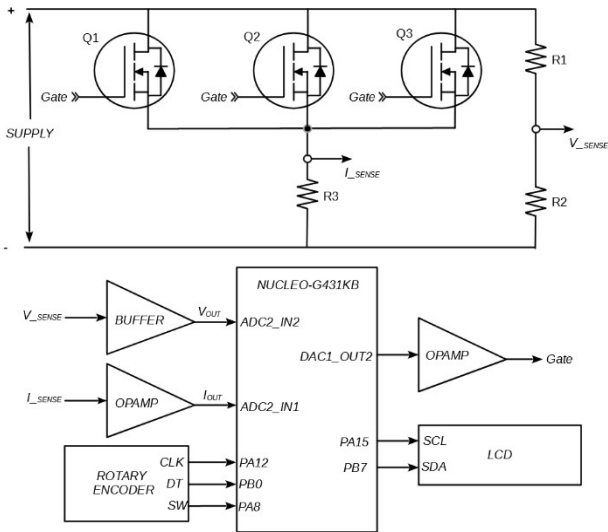


Fig. 1. System block diagram.

The mode of operation was selected using a push-button switch, and the reference value was configured using a rotary encoder. Upon selecting the mode, the microcontroller calculates the error between the measured values and set reference values. Based on this error, the gate voltage was adjusted by updating the digital to analog converter (DAC) output of the microcontroller. This DAC output was passed through a driver circuit to control the gates of the MOSFETs. As a result, MOSFETs act as variable resistors to generate the desired load. All measured data were logged via serial communication for further analysis and were also displayed on an I2C-based liquid crystal display (LCD) for real-time monitoring.

C. System Specifications

The programmable load was designed to support a maximum voltage of 100V and a maximum current of 50A with a total power handling capability of up to 300 W, ensuring that the current and voltage are within the permissible maximum limits. The unit can be used to validate and analyze a variety of power sources, including SMPS batteries, solar panels, and fuel cells, if they are within the design requirements.

III. METHODOLOGY

A 12V power supply was used to power the control circuitry of the system. This supply voltage is regulated to 5V and 3.3V by a voltage regulator [13, 14] to power the STM32 microcontroller and other circuit components. The STM32 microcontroller is a central controller that measures the system voltage and current. These signals were conditioned by op-amp-based amplifiers to ensure signal integrity and impedance matching.

The microcontroller processes these inputs and generates the corresponding control signals that are fed to a driver, which amplifies these signals to drive the gates of the three power MOSFETs. These MOSFETs act as controlled switches that dissipate power by allowing

current to flow through them.

An external switch is interfaced with the controller, enabling mode-selection functionality. Upon the first press, the LCD displays “Constant Current” mode. With subsequent presses, the display cycles through “constant voltage”, “constant power”, “constant resistance” and “energy source profiling” modes. Once a mode is selected, the user can set reference values by using the rotary encoder with the press of the encoder confirming the desired settings.

A. MOSFET Selection

In most applications, MOSFETs are operated as switches, with their operation occurring between the cut-off and Ohmic regions. However, in specific applications, such as battery testing, DC-DC converter testing, and programmable loads, MOSFETs are required to operate in the active (or saturation) region. In this region, the channel of the MOSFET becomes saturated with the majority charge carriers, and the drain current (I_D) becomes independent of the drain-source voltage (V_{DS}). Instead, I_D is solely determined by the gate-source voltage (V_{GS}), which remains constant for any given V_{DS} . This behavior causes the MOSFET to function as a constant-current sink. This characteristic makes the MOSFET ideal for use as a load, as it can precisely maintain a constant current, regardless of the applied voltage. This mode of operation is commonly referred to as the linear operation mode of a power MOSFETs. In linear mode, MOSFETs tend to dissipate higher power levels compared to their performance in switched-mode applications owing to the simultaneous presence of high voltage and current, leading to increased power dissipation [15].

The advantage of using MOSFETs in this mode for load applications is that it allows for a highly configurable and controllable load, making it possible to simulate various testing scenarios, such as constant current, constant voltage, or constant power profiles. This linear mode operation offers more precise and dynamic control over the load characteristics compared to traditional resistive loads, allowing for faster and more accurate testing of power electronics, including battery systems and DC-DC converters. Additionally, it reduces the complexity and physical limitations associated with adjusting resistive loads and enables more efficient and automated testing with the capability of handling higher power levels with less heat dissipation.

The forward bias safe operating area (FBSOA) is a datasheet figure of merit (FOM) that defines the maximum allowed operating points for safe operation. To ensure the safe operation of MOSFETs, it is essential to operate within the FBSOA limits, which are typically bounded by the RDS (ON) limit line, current, power, and voltage limit lines. Comparing standard MOSFETs with linear MOSFETs, linear MOSFETs offer an extended FBSOA, enabling them to handle higher power levels, particularly in applications that require both high voltage and current for extended periods.

Linear MOSFETs are designed to operate in the active (or linear) region, where they act as a constant-current sink, making them ideal for applications such as programmable loads and testing, where precise control over current is

necessary. In these applications, MOSFETs are typically used to regulate the current through the load, and are often arranged in parallel to handle higher power levels. Linear MOSFETs exhibit better performance than standard MOSFETs in such scenarios because they are capable of

handling higher power dissipation, particularly when subjected to conditions of high voltage and current for extended durations. This makes linear MOSFETs more suitable for linear-mode applications than their standard counterparts.

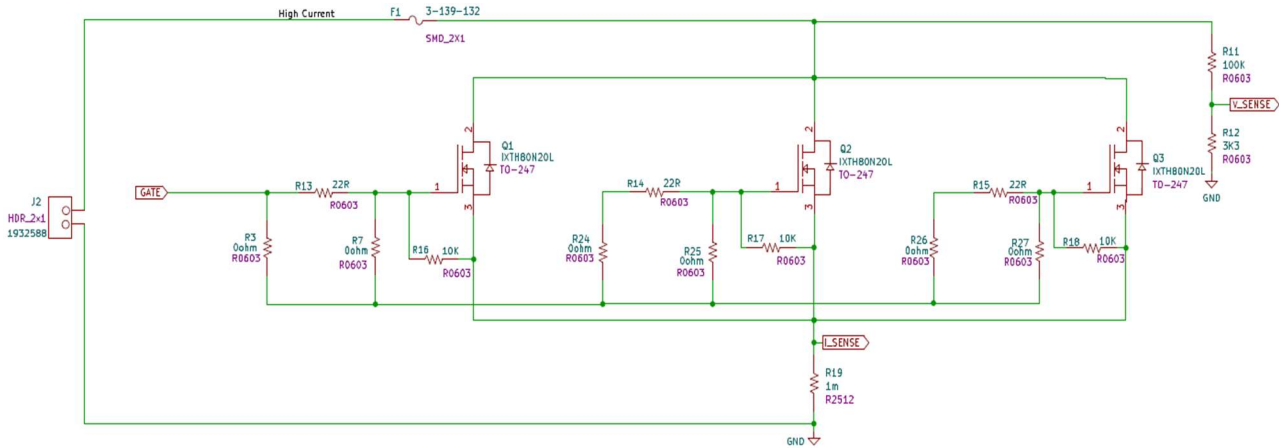


Fig. 2. Electronic load power circuit.

The linear MOSFET selected for this application is IXYS IXTH80N20L with drain to source voltage V_{DS} of 200V, drain current $I_D = 80A$ and Drain to Source on-state resistance $R_{DS(on)}$ of 32 mΩ which is designed to operate in the linear region for high-power applications. This MOSFET has the following key specifications [16]. The power circuit of electronic load employing three MOSFETs in parallel is shown in Fig. 2.

B. Microcontroller Selection

The microcontroller is the core of the system and is responsible for managing all operations. It must be capable of accurately measuring all the required parameters using a high-resolution ADC and DAC to ensure precise calculations. The microcontroller also needs to interface with components, such as the rotary encoder, LCD, ADC, and DAC. For this purpose, an STM32G431KBT6 microcontroller was selected. This microcontroller features the STM32G4 series in the UFQFPN32 package, which includes 128 kB flash memory and 32 kB SRAM. The microcontroller consists of 32 pins, providing the necessary I/O for the system components. In addition, it offers 12-bit digital-to-analog converters (DACs) that convert digital data into analog voltages. Each DAC module has two converters that operate synchronously or asynchronously. The microcontroller also includes a 12-bit internal ADC, enabling precise analog-to-digital conversion for accurate measurement of system parameters [17, 18].

C. Current and Voltage Measurements

The circuit features a voltage-sensing mechanism using a voltage divider network to measure the supply voltage and a shunt resistor of 1mΩ for current measurement, as shown in Fig. 3. An op-amp-based noninverting amplifier was employed to scale the voltage drop across the sense resistor to a range compatible with the ADC of the microcontroller [19]. A rail-to-rail op-amp ensures full utilization of the ADC input range, whereas a low input

offset voltage maintains accuracy when dealing with small signals. These conditioned voltage and current signals are fed to the microcontroller for precise control and monitoring [20].

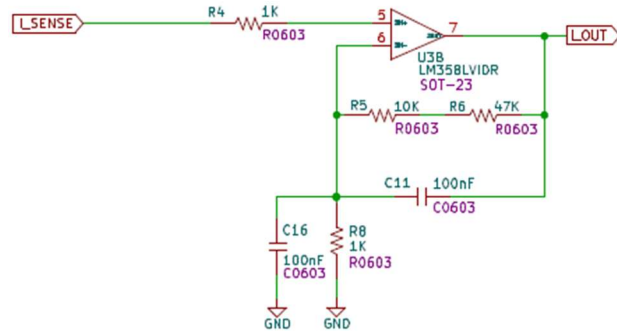


Fig. 3. Current measurement circuit.

In non-inverting configuration, the gain A_v is calculated as:

$$A_v = 1 + R_f/R_1 \tag{1}$$

Substituting the values for the feedback resistor $R_f=57k\Omega$ and $R_1=1k\Omega$. The gain of the op-amp was set to 58, enabling the accurate measurement of currents up to 57A accurately.

The voltage measurement circuit employed an operational amplifier (op-amp) in a voltage follower (buffer) configuration connected to a potential divider network, as shown in Fig. 4. The potential divider scales the input voltage to a level suitable for the microcontroller's ADC, whereas the buffer prevents loading effects and ensures accurate voltage measurement. The buffered output is then fed directly to the ADC input, enabling precise and reliable voltage monitoring.

The gate driver circuit, shown in Fig. 5, utilizes an LM358 operational amplifier to regulate the gate voltage of the MOSFET. The reference voltage generated by the DAC of the microcontroller was fed through this circuit to

the MOSFET gate. This ensures the precise operation of the MOSFET in its linear range, enabling accurate control of the current or voltage passing through the circuit.

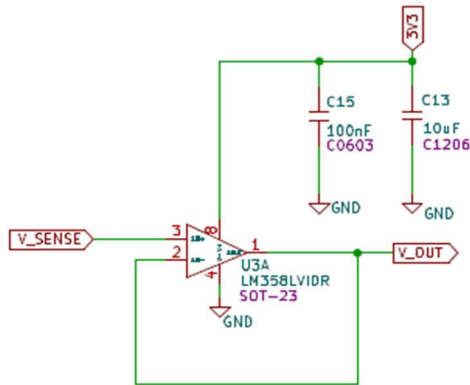


Fig. 4. Voltage measurement circuit.

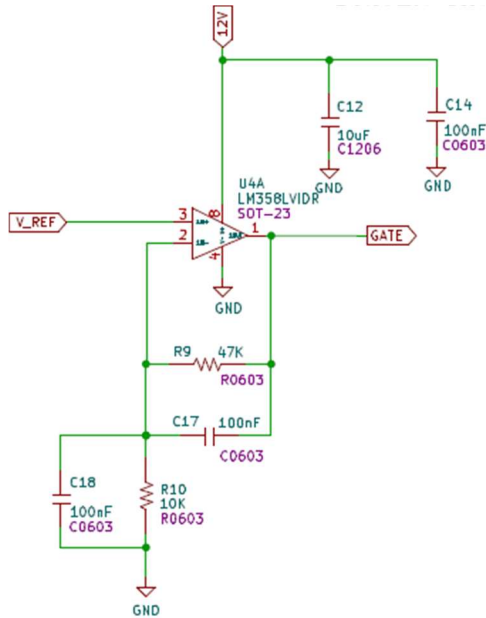


Fig. 5. Driver circuit.

D. Software Implementation

The software flow of the programmable load was designed to ensure seamless control, monitoring, and data logging for various operational modes, including constant current (CC), constant voltage (CV), constant resistance (CR), constant power (CP), and renewable energy source characterization, as shown in Fig. 6. The process begins with system initialization, in which all hardware peripherals, such as ADCs, DACs, and communication interfaces, are configured. Following initialization, the user selects the desired operational mode, which could be CC, CV, CR, CP, or Renewable Energy Source Characterization. Once the mode is selected, the system sets the corresponding reference values for parameters such as the current, voltage, resistance, or power, depending on the selected mode.

The software continuously monitors the voltage, current, and power readings using the ADC inputs. Based on the monitored parameters, the load was dynamically adjusted

to ensure that the reference values were maintained accurately. For modes such as Renewable Energy Source Characterization, additional logic handles variable input scenarios to evaluate the performance of the source. Throughout the operation, the system logged the data for subsequent analysis.

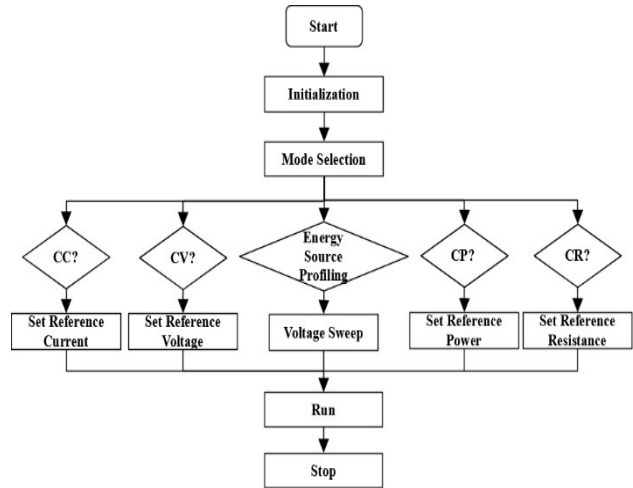


Fig. 6. System flowchart for mode selection and control.

The operational logic of the programmable load is executed within the Interrupt Service Routine (ISR) to ensure precise real-time control, as shown in Fig. 7. Upon initialization, the system begins by measuring current and voltage. These measurements are used to calculate resistance and power. Depending on the selected mode of operation (CC, CV, CP, or CR), the system computes the error between the set reference value and measured value. This error was then used to adjust the gate voltage of the FETs, and the corresponding DAC value was updated to maintain the desired operating conditions.

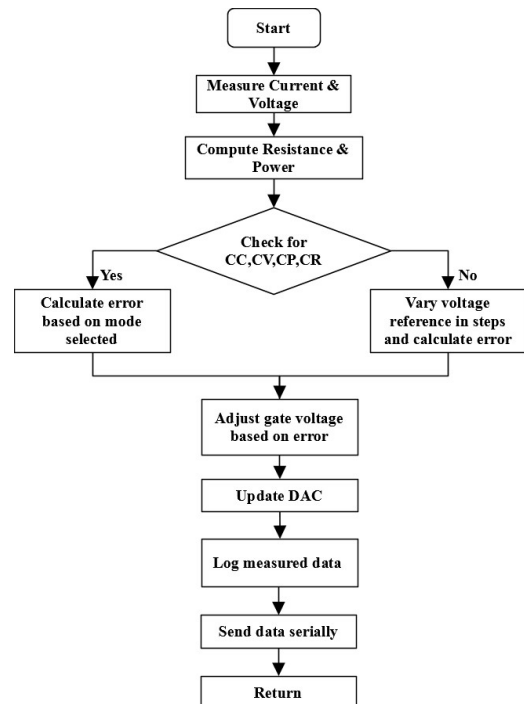


Fig. 7. Operational flowchart of programmable load.

For the characterization of the renewable energy source (RES), the voltage reference is varied in steps, and at each step, the error is computed and the DAC output is correspondingly updated. After data acquisition is complete, the recorded data are transmitted serially to Bluetooth, Wi-Fi, or a GSM connection for further analysis.

IV. RESULTS AND ANALYSIS

A. Hardware Setup

The schematic and PCB layout of the unit were prepared using KiCad 7.0, a Schematic Editor and PCB Editor tools. The developed unit had dimensions of 15 cm × 10 cm and was fabricated as a 2-layer PCB as shown in Fig. 8. The final unit after the component soldering and assembly is shown in Fig. 9.

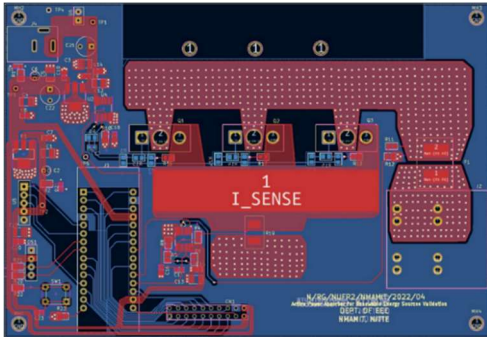


Fig. 8. PCB layout of the developed unit.



Fig. 9. Hardware prototype of developed unit.

B. Hardware Results

1) To validate DC-DC buck converter

The developed programmable load was configured in different modes to validate the performance of a 12 V to 9 V, 12 W DC-DC buck converter, as shown in Fig. 10. The programmable load was utilized in constant-current, constant-resistance, and constant-power modes to conduct a comprehensive analysis of the buck converter's performance under diverse loading conditions.



Fig. 10. Experimental set-up to validate DC-DC buck converter.

In the constant current mode, the e-load was programmed to maintain a reference current of 1A. The buck converter was evaluated across a duty cycle ranging from 0% to 100%, and its output voltage and current were measured under these conditions and tabulated in Table I. Irrespective of the load voltage, the unit dynamically adjusts its resistance to maintain the programmed current with a deviation of only 0.01A, thereby ensuring stable load conditions for accurate performance evaluation of the converter.

In the constant resistance mode, a reference resistance of $R_{set}=10\Omega$ was selected. The output voltage was varied incrementally, and at each step, the unit adjusts the current to maintain the programmed resistance value. The results show that for light loads, a significant error was observed. However, as the load increases, the error decreases, remaining within 2% as in Table II.

TABLE I: RESULT OF CONSTANT CURRENT MODE

Duty cycle (%)	Output voltage (V)	Output current (A)
40	3.59	1.01
50	4.89	1.01
60	6.12	1.01
80	8.72	1.01
100	11.29	1.01

TABLE II: RESULT OF CONSTANT RESISTANCE MODE

Output voltage (V)	Output current (A)	Output resistance (Ω)	% Error $\frac{R_{set}-R}{R_{set}} \times 100$
2.03	0.19	10.68	-6.8%
4.06	0.4	10.15	-1.5%
6.27	0.63	9.95	0.5%
8.06	0.8	10.075	-0.75%
10	1.01	9.9	1%

TABLE III: RESULT OF CONSTANT POWER MODE

Output voltage (V)	Output current (A)	Output power (W)	% Error $\frac{P_{set}-P}{P_{set}} \times 100$
4.08	1.44	5.88	2%
6.08	0.98	5.96	0.66%
8.05	0.75	6.04	-0.66%
10.03	0.61	6.11	-1.83%
11.33	0.54	6.11	-1.83%

The percentage error in resistance, is calculated using $\frac{R_{set}-R}{R_{set}} \times 100$ that quantifies the deviation of the actual resistance R from the set resistance R_{set} in constant resistance mode operation in normalized measure of accuracy. A positive percentage error indicates that the actual resistance is lower than the set value, while a negative error signifies an actual resistance higher than the intended value.

In constant power mode, the e-load was configured with a reference power of $P_{set} = 6W$. The output voltage was varied incrementally, and at each step, the load adjusted the sink current to absorb the programmed power. From the results as in Table III, it can be seen that the error was within 2%.

The percentage error in constant power mode is calculated using $\frac{P_{set}-P}{P_{set}} \times 100$ were, P_{set} is the set value of power and P is the actual output power.

2) Characterization of PV panel

In this mode of operation, 250 samples of the PV current, voltage, and power were collected, completing the data acquisition within 25 s. This rapid and automated process enables accurate plotting of I-V and P-V curves without human intervention. Unlike conventional methods, where the resistance is varied manually over a prolonged period, this approach eliminates the risk of irradiance changes that affect the accuracy of the PV curves. By automatically varying the resistance every 100 ms, the system minimizes the errors and inefficiencies associated with manual measurements, ensuring precise and reliable results. The system setup is shown in Fig. 11.

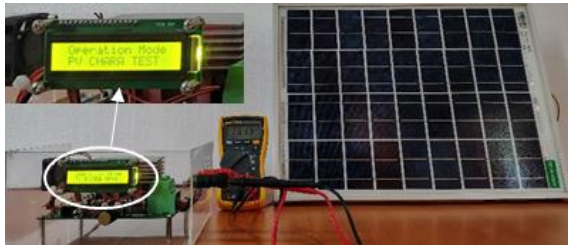


Fig. 11. Experimental set-up to plot IV & PV curves of panel.

The characterization of the PV panel was conducted on a 75 W panel [21] using natural sunlight at different times of the day to record readings under varying irradiance levels, as in Fig. 12 and Fig. 13. The maximum power point (MPP) power, current, and voltage values for each irradiance level are summarized in Table IV, providing detailed insights into the panel's performance under different irradiance conditions.

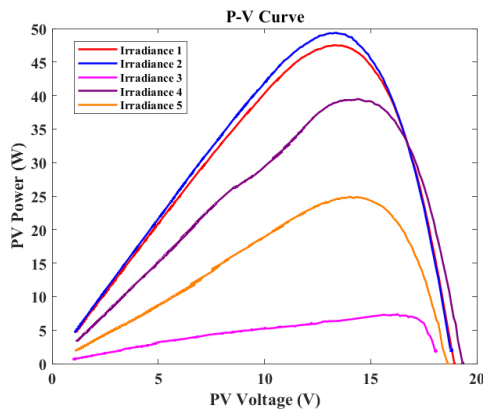


Fig. 12. P-V curves of 75W panel under different irradiances.

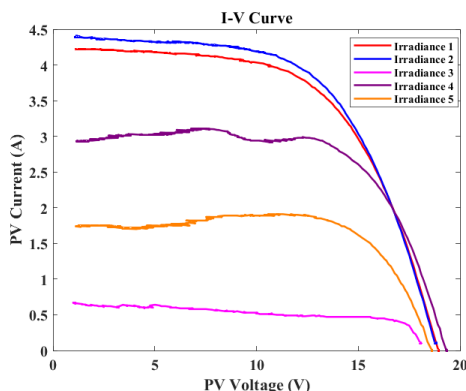


Fig. 13. I-V curves of 75W panel under different irradiances.

The non-monotonic trends in Fig. 13 are due to fluctuations in natural sunlight, as the readings were taken under varying outdoor conditions. Changes in irradiance due to passing clouds, atmospheric variations, or shifts in the sun's position throughout the day may have introduced slight deviations in the I-V and P-V curves.

TABLE IV: PERFORMANCE METRICS OF PV PANEL UNDER DIFFERENT IRRADIANCE LEVELS

Irradiance level	V_{mp} (V)	I_{mp} (A)	P_{mp} (W)
Irradiance 1	13.32	3.57	47.55
Irradiance 2	13.38	3.69	49.37
Irradiance 3	15.65	2.65	7.33
Irradiance 4	14.40	2.74	39.46
Irradiance 5	14.31	1.74	24.90

V. CONCLUSION

This study presents the design and implementation of a programmable load solution to address the challenges of testing and validating renewable energy systems, battery technologies, and DC power sources. This work includes detailed discussions on hardware and software implementation, along with component selection to ensure precision and reliability. The system supports operation in Constant Current (CC), Constant Power (CP), and Constant Resistance (CR) modes, making it suitable for testing DC-DC converters and other power systems. Additionally, PV panel characterization under different irradiance conditions was performed, with I-V and P-V curves were plotted to demonstrate the system functionality. All acquired data were logged via serial communication, enabling a comprehensive future analysis.

By incorporating features such as real-time data logging, remote monitoring, and automated control, the system significantly reduces the testing time and costs while maintaining accuracy and repeatability. The integration of safety features such as overcurrent and overvoltage protection ensure reliability during operation. The programmable load effectively emulates real-world load conditions, providing a versatile and robust platform for testing power electronic systems, particularly DC-DC converters and renewable energy sources, ensuring improved performance, quality, and reliability.

Future enhancements can focus on increasing the voltage and current handling capabilities to support a wider range of power sources. The implementation of adaptive control algorithms, such as machine learning-based strategies, can further optimize real-time response and efficiency.

CONFLICT OF INTEREST

The authors declare no conflict of interest.

AUTHOR CONTRIBUTIONS

Swathi Hatwar H. drafted the manuscript and contributed to the hardware design and development. Anup Shetty was responsible for developing the hardware setup, software implementation, and obtaining the results. Suryanarayana K. was responsible for conceptualizing the idea, providing guidance, and supervising the research. All

authors reviewed and approved the final version of the manuscript.

FUNDING

This research was funded by Nitte (Deemed to be University), Nitte Education Trust, grant number N/RG/NUFR2/NMAMIT/2022/04.

ACKNOWLEDGMENT

The authors would like to thank NMAM Institute of Technology, Nitte, Karkala, for providing a platform to carry out work at the Research & Innovation Center. The authors would also like to thank the students Nireeksha Alva, Nishmitha S Kotian, Rakshitha Shetty, and S S Ananya for their support during prototype development.

REFERENCES

- [1] L. F. Serna-Motoya, J. R. Ortiz-Castrillón, P. A. Gil-Vargas *et al.*, "Implementation of a programmable electronic load for equipment testing," *Computers*, vol. 11, no. 7, p. 106, Jul. 2022.
- [2] M. S. Khan, C.-H. Lin, J. Ahmad *et al.*, "A novel DC electronic load topology incorporated with model predictive control approach," *Mathematics*, vol. 11, no. 15, p. 3353, 2023.
- [3] A. Asbayou, M. Agdam, A. Aamoume *et al.*, "Utilization of MOSFET transistor as an electronic load to trace I-V and P-V curve of a solar panel," in *Proc. E3S Web Conf.*, 2021. doi: 10.1051/e3sconf/202122901021
- [4] Q. Yang, Y. Zhang, T. Li *et al.*, "Wide input voltage DC electronic load architecture with SiC MOSFETs for high efficiency energy recycling," *IEEE Trans. Power Electron.*, vol. 35, no. 12, pp. 13053–13067, Dec. 2020.
- [5] W. Jin, Y. Fu, M. Li *et al.*, "High-precision programmable electronic load for I-V characteristic simulation," in *Proc. 2024 IEEE 19th Conf. Ind. Electron. Appl. (ICIEA)*, Kristiansand, Norway, 2024. doi: 10.1109/ICIEA61579.2024.10665152
- [6] A. Ria, G. Manfredini, F. Gagliardi *et al.*, "Online high-resolution EIS of lithium-ion batteries by means of compact and low power ASIC," *Batteries*, vol. 9, no. 5, 2023.
- [7] Keysight Technologies, "Electronic load fundamentals," *White Paper*, Jun. 20, 2022, pp. 1–12, Document no. 5992-3625EN.
- [8] W. Saksiri, P. Akarach *et al.*, "DC constant current electronic load: Stability analysis," in *Proc. 2024 1st Int. Conf. Robot., Eng., Sci., Technol. (RESTCON)*, Pattaya, Thailand, 2024, pp. 69–73.
- [9] M. M. G. Costa, K. M. M. Damasceno, E. Nepomuceno *et al.*, "Modeling and design of a low-cost constant current electronic load," in *Proc. 2023 15th Semin. Power Electron. Control (SEPOC)*, Santa Maria, Brazil, 2023, pp. 1–6. doi: 10.1109/SEPOC58810.2023.10322628
- [10] K. Kumar, "Design and realization of programmable electronic load for aerospace vehicle testing," in *Proc. 2024 IEEE Space, Aerospace and Defence Conf. (SPACE)*, Bangalore, India, 2024, pp. 108–111. doi: 10.1109/SPACE63117.2024.10667846
- [11] A. Asbayou, A. Aamoume, M. Elyaqouti *et al.*, "Benchmarking study between capacitive and electronic load technic to track I-V and P-V of a solar panel," *Int. J. Electr. Comput. Eng. (IJECE)*, vol. 12, no. 1, pp. 102–113, 2022.

- [12] A. Asbayou, M. Agdam, A. Aamoume *et al.*, "Utilization of MOSFET transistor as an electronic load to trace I-V and P-V curve of a solar panel," *E3S Web Conf.*, vol. 229, 2021. doi: 10.1051/e3sconf/202122901021
- [13] On Semiconductor, "1.0 A low-dropout positive fixed and adjustable voltage regulators," *Datasheet*, 2021.
- [14] Texas Instruments, "LM340, LM340A and LM7805 family wide VIN 1.5-A fixed voltage regulators," *Datasheet*, 2023.
- [15] J. Padilla, "Understanding linear MOSFETs and their applications," *Technical Article*, 2021.
- [16] IXYS Corporation, "Linear power MOSFET w/ extended FBSOA (IXTH80N20L)," *Datasheet*, 2021.
- [17] STMicroelectronics, "STM32G431KBT6," *Datasheet*, 2022.
- [18] STMicroelectronics, "STM32G4 Nucleo-32 board (MB1430)," *User Manual*, 2022.
- [19] Texas Instruments, "LMV3xx low-voltage rail-to-rail output operational amplifier," *Datasheet*, 2023.
- [20] Renesas Electronics, "Current sensing with low-voltage precision op-amps," *Application Note*, 2022.
- [21] BP Solar India Limited, "Model number: TBP1275M," *Technical Specifications*, 2023.

Copyright © 2025 by the authors. This is an open access article distributed under the Creative Commons Attribution License ([CC BY 4.0](https://creativecommons.org/licenses/by/4.0/)), which permits use, distribution and reproduction in any medium, provided that the article is properly cited, the use is non-commercial and no modifications or adaptations are made.



electronics, control systems.

Swathi Hatwar H. is working as an assistant professor in the Department of Electrical & Electronics Engineering, NMAM Institute of Technology, Nitte, Karkala, Karnataka since 14 July 2014. She received her M.Tech. degree from NMAMIT, Nitte in 2014. Presently, she is pursuing her Ph.D. study from Visveswaraya Technological University Belagavi. Her area of interests are embedded systems, power



Anup Shetty is working as an assistant professor in the Department of Electrical & Electronics Engineering, NMAM Institute of Technology, Nitte, Karkala, Karnataka since 01 July 2022. He received his M.Tech. degree from NMAMIT, Nitte in 2020. His area of interests are embedded systems, power electronics, control systems.



Suryanarayana K. is working as a professor in the Department of Electrical & Electronics Engineering, NMAM Institute of Technology, Nitte, Karkala, Karnataka since 1 July 2022. He received his Ph.D. degree from Visveswaraya Technological University Belagavi in 2017. He has worked in industries for ten years. His interests are signal processing, power electronics, control systems. He is member of IEEE.